Cryogenic All Solid-State Millimeter-Wave Receivers for Airborne Radiometry

BERND VOWINKEL, KONRAD GRUENER, AND WERNER REINERT

Abstract—**Cryogenic receiver modules for 90 and 140 GHz have been developed that are part of an airborne imaging system. They consist of Schottky-barrier mixers followed by GaAs-FET IF amplifiers. The DSB receiver noise temperatures are 210 K for the 90-GHz and 250 K for the 140-GHz system. The instantaneous bandwidth is 2.5 GHz for both front ends. Results of some flight tests are presented.**

I. Introduction

HIGH-RESOLUTION airborne microwave imaging is of great practical interest for the remote sensing of the earth's surface. In particular, the millimeter-wave region is very useful because higher angular resolution can be achieved with small antennas and, at the same time, contrast losses due to weather conditions and atmospheric attenuation are still small. In the past, however, the resolution of millimeter-wave airborne imaging systems was very limited because of the relatively high noise temperatures of the uncooled receivers used. This resulted in data rates on the order of only 100 samples per second for a temperature resolution of 1 K [1]. In order to increase this value by at least one order of magnitude, cryogenic receiver front ends for 90 and 140 GHz have been developed that have extremely low noise temperatures and very broad instantaneous bandwidths [2].

II. Receiver Concept

In order to avoid the inherent resolution losses of a Dicke system or a correlation system, the simple total-power receiver concept was chosen, where the receiver input is always connected to the antenna [3]. The disadvantage of the uncompensated gain fluctuations in a total-power system was found to be negligible in our case, because of the short integration times used (on the order of milliseconds). In addition, the short- and long-term stability of the receiver was improved by temperature control of all critical components (IF-amplifiers, detector, etc.).

Fig. 1 shows a block diagram of the receiver. Two exchangeable cryogenic front-end modules have been built, one for 90 GHz and the other one for 140 GHz. They consist of a Schottky-barrier mixer followed by a two-stage IF-amplifier. A closed cycle refrigerator system (CTI 21) is used to cool the modules down to 20 K. The weight of the compressor is 39 kg and the power consumption is 1.1 kW. The cooled components are located in a vacuum chamber, in order to prevent thermal heating due to convection and condensation of the air. The available cryogenic power at 20 K is about 1.5 W, so that the heat input due to the dc-power dissipation in the transistors (25 mW per transistor) is negligible. The main heat power input is caused by the heat conduction of the waveguide connection between the mixer and the local oscillator. For this reason, a stainless-steel waveguide with low heat conductivity was used for the 90-GHz system. For the 140-GHz system, a silver waveguide had to be used because of the lower attenuation compared to stainless steel. In order to reduce the heat-conduction cross section, the waveguide walls have been thinned to a thickness of 0.4 mm.

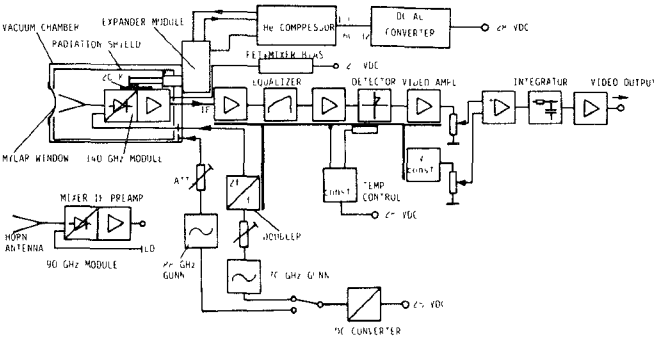

Fig. 1. Block diagram of the receiver.

The mixers are pumped by Gunn-oscillators. For the 140-GHz receiver module, a 70-GHz Gunn-oscillator followed by a frequency doubler is used. Fig. 2 shows a cross-sectional view of the doubler. The efficiency is about 10 percent, giving an available output power of 2 mW at 140 GHz. The diode used is of the same type as the diodes used for the mixers. Special varactor diodes would result in a much better efficiency [4]; however, the pump-power requirement of the mixer was only about 0.1 mW when cooled to 20 K, therefore, there was no need for a further improvement of the doubler.

The IF-signal from the cryogenic front end is further amplified and then rectified in a back-diode detector. An amplitude equalizer is inserted to smooth the frequency response of the IF-amplifier chain. Fig. 3 shows the compensated frequency response. The IF-band limits of 1.5 and 4 GHz, respectively, are defined by the gain dropoffs

Manuscript received March 25, 1983; revised August 4, 1983.

B. Vowinkel is with I.Physikalisches Institut der Universitaet Koeln, Universtaetsstrasse 14, D-5000 Koeln 41, Federal Republic of Germany.

K. Gruener is with DFVLR, Institut fuer HF-Technik, D-8031 Oberpfaffenhofen, Federal Republic of Germany.

W. Reinert is with Institut fuer Angewandte Festkoerperphysik, Eckerstrasse 4, D-7800 Freiburg, Federal Republic of Germany.

0018-9480/83/1200-0996$01.00 ©1983 IEEE

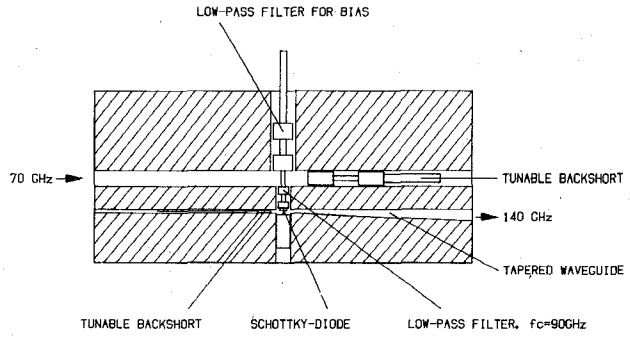

Fig. 2. Cross-sectional view of the doubler.

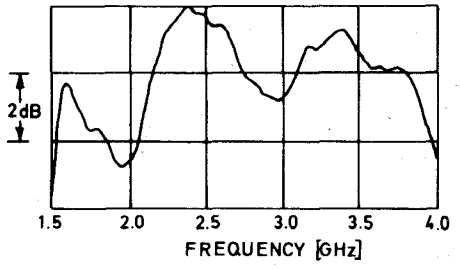

Fig. 3. IF-gain response of the receiver.

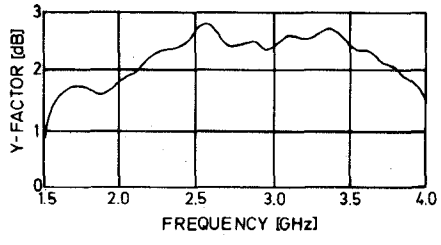

Fig. 4. *Y*-factor versus intermediate frequency.

of the amplifiers. The DSB receiver noise temperatures have been measured by the hot/cold method, using absorber material at room temperature and at liquid nitrogen temperature, that is alternately placed in front of the horn antenna. Fig. 4 shows the frequency response of the resulting *Y*-factor ($P_{\text{hot}}/P_{\text{cold}}$) for the 90-GHz module. The degradation towards the lower and upper IF-band limits is mainly caused by the increasing mismatch between the mixer IF-output and the input of the first IF-preamplifier stage.

III. Front-End Modules

A cross-sectional view of the 90-GHz front-end module is shown in Fig. 5. The 140-GHz module looks quite similar to this. The local oscillator is coupled via a TE_{111}-mode cavity filter into the signal waveguide, which is an electroformed transition to a reduced height (1/3) waveguide cross section. Due to the bandpass frequency response of the filter, the signals in both sidebands of the mixer are reflected at the filter. Therefore, at the signal frequencies, the filter acts as a backshort. The distance between filter and mixer diode was experimentally optimized for minimum noise figure.

The mixer diodes have been fabricated at the Institut fuer Angewandte Festkoerperphysik in Freiburg, West

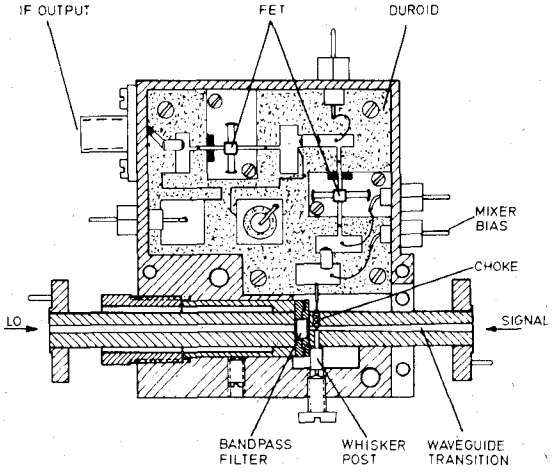

Fig. 5. Cross-sectional view of the 90-GHz front-end module.

Germany. The diameters of the Schottky contacts are 2 μm and the epilayer doping concentration is $2 \cdot 10^{16}$ cm^{-3}. The parasitic series resistance is 7 Ω and the ideality factor (characteristically inverse slope of *V*-log *I* curve) is 1.07 at room temperature. This type of diode is used for both front-end modules.

The cryogenic IF amplifiers have been optimized for the frequency band from 1.5 to 4 GHz, resulting in a noise temperature of 35 K for the IF-amplifier chain. The gain is 12 dB per stage. In order to reduce the uncooled post-amplifier noise contribution, two stages are mounted in each front-end module. The transistor-type MGF 1412 (Mitsubishi) was used for all cryogenic amplifier stages. For the input and output matching networks, double-section matching transformers in microstrip technology have been chosen. In order to achieve a broad matching bandwidth, short (0.1 λ) matching elements were used [5]. The same technique was applied for the matching of the mixer IF-output port. For the calculation of the matching elements, the room-temperature *S*-parameters of the transistors have been taken. The only *S*-parameter that changes considerably when the transistor is cooled to 20 K is S_{21}, resulting in a gain increase of about 1 dB compared to the room-temperature performance. This gain increase can cause high-frequency oscillations. In order to avoid this, small pieces of ferrite absorber material were glued underneath the drain leads of the transistors [6].

Table I gives a summary of the specifications of both front-end modules. The stated figures for the theoretical data rate are calculated for a temperature resolution of 1 K, assuming a mean value for the antenna temperature of 250 K. However, the real values for the complete imaging system are about 40 percent lower because of the nonideal frequency response of the IF-amplifier chain (see Fig. 3), radome losses, and the limited main-beam efficiency of the antenna.

IV. Imaging System

The cryogenic receiver is part of an airborne imaging system. The two front-end modules can be exchanged within a short time. However, the cryogenic part of the

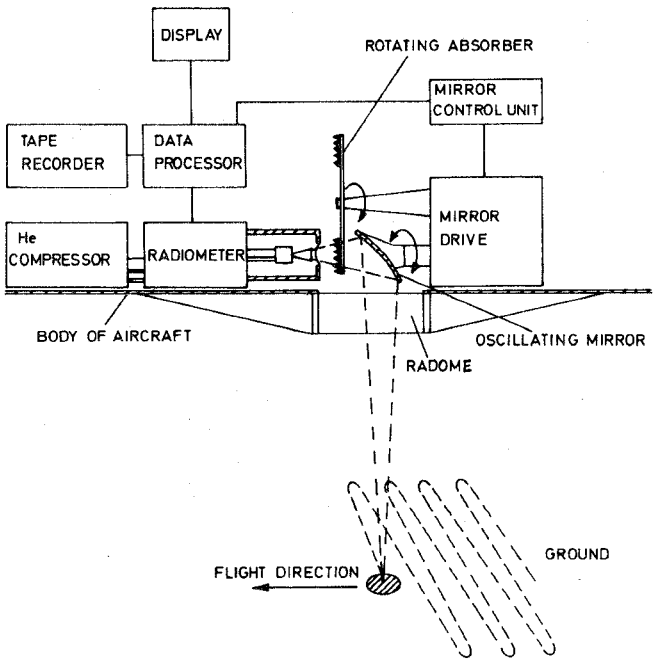

Fig. 6. Block diagram of the imaging system.

TABLE I
SPECIFICATIONS OF THE RECEIVER FRONT ENDS

center frequency	88 GHz	140 GHz
intermediate frequency	1.5-4 GHz	1.5-4 GHz
IF bandwidth	2.5 GHz	2.5 GHz
receiver noise temp. (DSB) at room temp.	710 K	870 K
receiver noise temp. (DSB) at 20 K	210 K	250 K
theor. data rate (1 K)	11815 s^{-1}	10000 s^{-1}
stability, short term	$3 \cdot 10^{-5}$/min	$3 \cdot 10^{-5}$/min
stability, long term	$2 \cdot 10^{-4}$/h	$2 \cdot 10^{-4}$/h

receiver has to be at room temperature for the exchange. The cool-down time is about 3.5 h. At both frequencies, the same off-axis parabolic mirror antenna is used. The minor axis diameter is 20 cm, giving an angular resolution (half-power beamwidth) of about 1° at 90 GHz and 0.7° at 140 GHz. The antenna oscillates around an axis parallel to the flight direction so that the ground is scanned perpendicular to the flight path (see Fig. 6). The maximum oscillation frequency is 38.5 Hz and the scan angle is ±14.5°. In order to achieve this relatively high oscillation frequency, the mirror has been made of carbon-fiber reinforced epoxy, which results in a weight of only 63 g for the mirror.

For absolute temperature calibration, a rotating absorber is placed between the mirror and the receiver input.

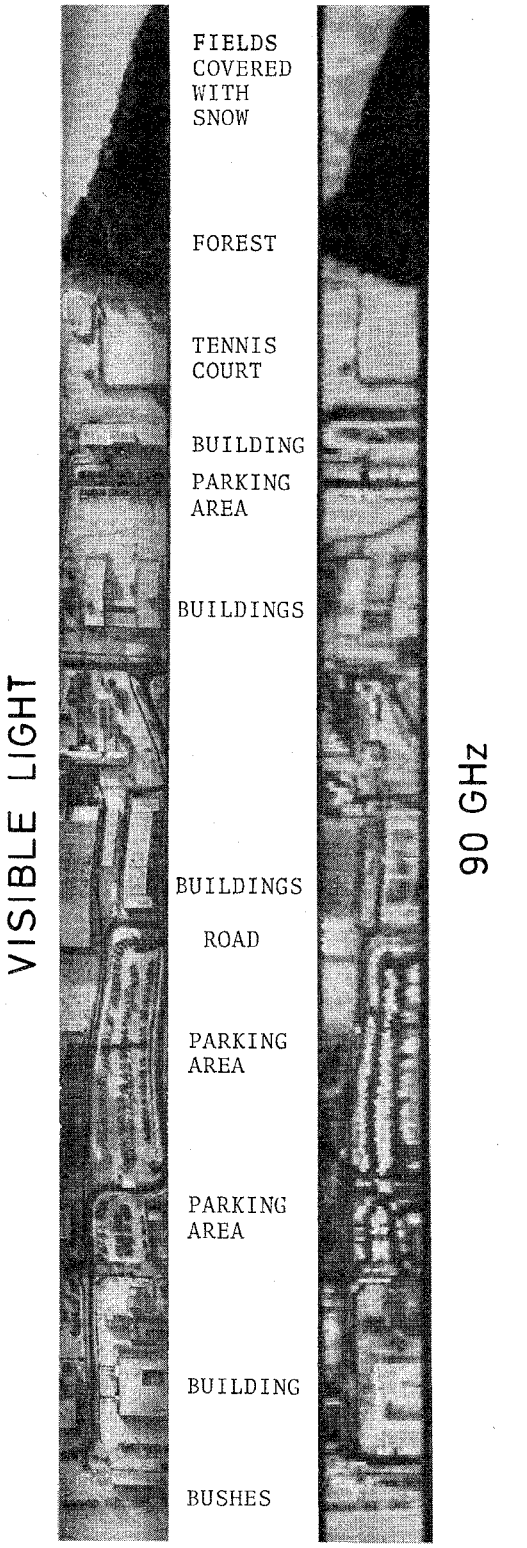

Fig. 7. DFVLR area, altitude: 85 m, comparison: visible light (left) with 90-GHz image (right). Dark areas have a higher radiometric temperature in the 90-GHz image.

The dumbell-shaped absorber is synchronized with the mirror such that it covers the receiver input when the mirror changes the direction of movement. The data are recorded on magnetic tape for further analysis on the ground and also are displayed on a screen for quick-look evaluation.

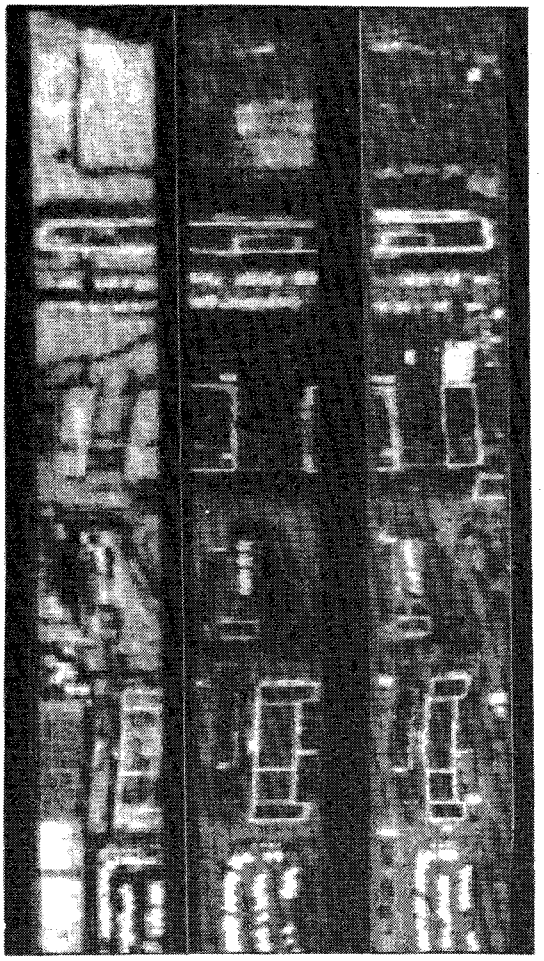

Fig. 8. Central part of Fig. 7 at 90 GHz in wintertime (left), 90 GHz in summertime (middle), and 140 GHz in summertime (right).

V. Results

The imaging system has been flown several times aboard a small twin-engine aircraft (Dornier Do 28). Fig. 7 shows a 90-GHz image of the DFVLR area, taken from an altitude of 85 m. A visual photograph of the same area is shown on the left for comparison. The shown area of 43 by 650 m was overflown within 13 s (aircraft speed: 50 m/s). The central part of the area is shown again in Fig. 8 at 90 GHz (left and middle) and 140 GHz (right). The 90-GHz image at left was taken in wintertime, whereas the two other images were taken in summertime. The snow cover can be clearly identified when comparing the images. Fig. 9 shows airplanes parked on a concrete platform at 90 GHz (left) and 140 GHz (right). In both pictures small vehicles around the airplanes can also be detected. Furthermore, radiometer resolution is sufficiently fine to display the substructure of the concrete platform.

Fig. 10 exemplifies the capability of high-resolution microwave radiometry under bad weather conditions. The flight path runs from top left to bottom middle and shows in the first part a highway with exit and access roads. Several cars can be identified (white pixels) on the highway. The flight path then passes over snow-covered fields (middle) to a small village (bottom middle). The four

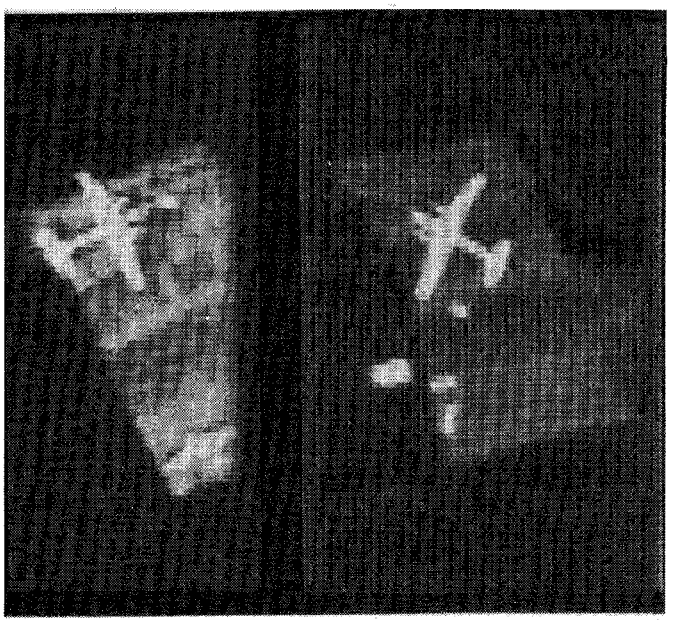

Fig. 9. 90-GHz (left) and 140-GHz images of airplanes. Altitude: 85 m. Scanwidth: 45 m.

Fig. 10. 90-GHz image at degrading ground visibility. The flight path runs from top left to bottom middle. The four pictures at right show the ground at visible light. Altitude: 100 m. Total length of shown area: 1500 m. Scanwidth: 53 m.

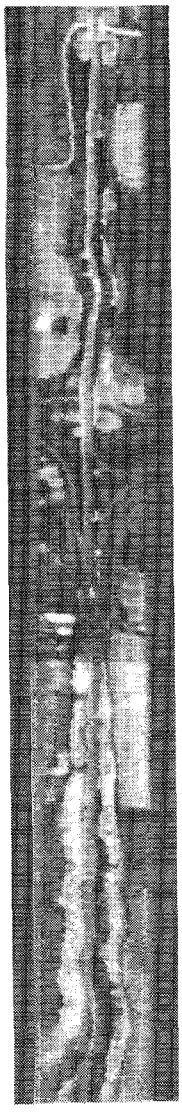

Fig. 11. First section of Fig. 10 at 140 GHz in summertime. The gray scale ranges from an antenna temperature of 270–292 K.

pictures shown at right were taken with a CCD-camera at visible wavelengths. The upper three pictures were taken above the highway and the last one above the village. These pictures show the degrading ground visibility along the flight path. However, in the 90-GHz image no contrast loss can be observed. Also, the trail of smoke which can be seen at the bottom of the second CCD image is invisible in the 90-GHz image. Fig. 11 shows the first part of the flight path again at 140 GHz (in summertime). In this image, different kinds of vegetation can be clearly distinguished. The contrast of roads, however, is much smaller compared to the 90-GHz images.

The contrasts of different kinds of vegetation are relatively small in the millimeter-wave region so that a temperature resolution of at least 1 K is necessary to obtain well-structured images. Fig. 12 shows, for example, imagery of vegetation of 90 (left) and 140 GHz (right). The 140-GHz image was taken from a higher altitude (128 m) so that the spatial resolution is comparable for both images. The scene contains two different cornfields and a forest with conifers (bottom), and deciduous trees. The timberline

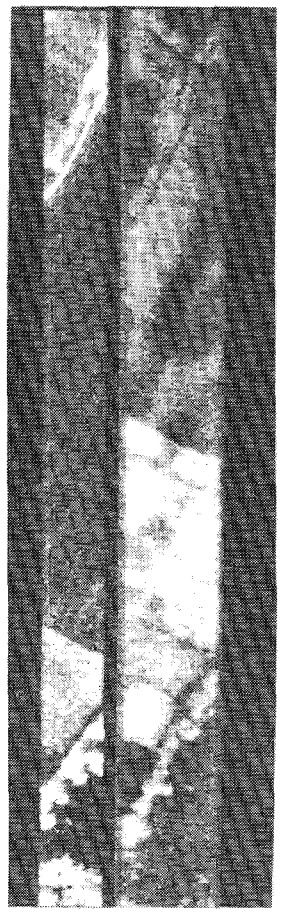

Fig. 12. 90-GHz (left) and 140-GHz (right) images of a section with different types of fields and a forest (bottom). Altitude: 85 m (90 GHz) and 128 m (140 GHz).

passes diagonally through the picture. The 140-GHz image was taken one year later, which is the reason for some changes of the vegetation. In general, images at 140 GHz have a lower contrast compared to images at 90 GHz, because of the higher radiometric temperature of the sky at 140 GHz.

VI. Future Developments

For an improvement of the available data rate, a further reduction of the receiver noise temperature is of very limited value, because the contribution to the total system noise temperature is only about 50 percent for the present receiver front ends, assuming an antenna noise temperature around 250 K. Even a noise-free receiver would lead to an improvement in the data rate of only a factor of 4. The only way to further increase the data rate by orders of magnitude is, therefore, the development of multichannel receivers and an improvement of the instantaneous bandwidth.

A further resolution-limiting component in the current design is the oscillating mirror. For an improvement of the spatial resolution, a larger mirror and a higher mirror oscillation frequency would be necessary. These, however, are contrary requirements, because a larger mirror has a higher moment of inertia and thus must be operated at a lower oscillation frequency.

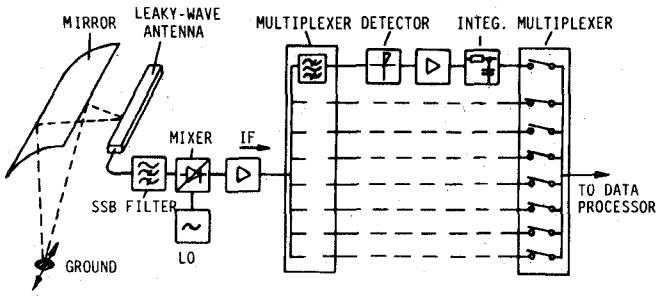

Fig. 13. Schematic diagram of new imaging concept.

In order to avoid the problems caused by the mechanically movable mirror, a new imaging system concept has been studied. In this concept the oscillating mirror is replaced by a combination of a leaky wave antenna with a cylinder-parabolic mirror (see Fig. 13). When the leaky wave antenna is operated close to the cutoff frequency of the waveguide, the angle between the main beam and the waveguide gets strongly frequency dependent. Thus the scanning in one direction can be performed by measuring at different receiving frequencies.

The signal coming from the antenna is converted down to an IF of 2–8 GHz. This broad IF-band is then amplified in a low-noise amplifier and split into a number of different frequency bands in a multiplexer circuit. The signals in the bands are then separately rectified, preintegrated, and further processed. Each channel corresponds to a different main-beam angle, so that the ground is scanned with parallel beams separated by a half-power beam width. Nonlinearities in the main-beam angle to frequency dependence can be compensated for by adjusting the instantaneous bandwidths of the corresponding IF-channels.

One disadvantage of the described system is that the mixer has to be operated in the SSB mode, which increases the effective noise temperature compared to conventional DSB imaging receivers. This, however, will be partly compensated for by the relatively broad effective bandwidth of 6 GHz. Low-noise amplifiers with a noise figure of less than 5 dB are commercially available for this frequency band. As there may be problems in covering a larger total scan angle of, say, 30° with a resolution of about 1° (at 90 GHz), several separate leaky wave antennas with complete receiver systems may be put together in the focus line of the mirror, where each antenna covers a different part of the total scan angle.

Acknowledgment

The authors wish to thank K. Jacobs for the fabrication of the diode whiskers and H. Schreiber, G. Kahlisch, G. Griebel, and P. Vogel for the mechanical construction of the mirror drive, the antenna reflector, and the installation and operation of the system.

References

[1] J. P. Hollinger, J. E. Kenney, and B. E. Troy, "A versatile millimeter wave imaging system," *IEEE Trans. Microwave Theory Tech.*, vol. MTT-24, pp. 786–793, Nov. 1976.

[2] B. Vowinkel, J. K. Peltonen, W. Reinert, K. Gruener, and B. Aumiller, "Airborne imaging system using a cryogenic 90-GHz receiver," *IEEE Trans. Microwave Theory Tech.*, vol. MTT-29, pp. 535–541, June 1981.

[3] G. Evans and C. W. McLeish, *Radiometer Handbook*, Dedham, MA: Artech House, 1977.

[4] J. W. Archer, "Millimeter wavelength frequency multipliers," *IEEE Trans. Microwave Theory Tech.*, vol. MTT-29, pp. 552–557, June 1981.

[5] B. Vowinkel, "Cryogenic 2–4 GHz FET amplifier," *Electron. Lett.*, vol. 16, no. 19, pp. 730–731, Sept. 1980.

[6] S. Weinreb, D. L. Fenstermacher, and R. W. Harris, "Ultra-low-noise 1.2- to 1.7-GHz cooled GaAsFET amplifiers," *IEEE Trans. Microwave Theory Tech.*, vol. MTT-30, pp. 849–853, June 1982.

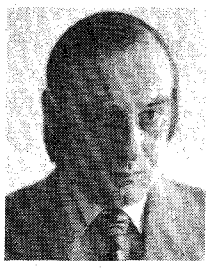

Bernd Vowinkel was born in Alsfeld, West Germany, on May 15, 1947. He received the Ing. (grad.) degree in electrical engineering from Fachhochschule Giessen, Giessen, West Germany, in 1968, and the Diplom-Physiker and Dr. degrees from the University of Bonn, Bonn, West Germany, in 1975 and 1978, respectively.

From 1968 to 1970, he was employed at a satellite tracking station of the European Space Agency. From 1975 to 1981, he was with the Radioastronomisches Institut of the University of Bonn, where he was concerned with the development of low-noise millimeter-wave receiver systems. Since 1981, he has been with the I.Physikalisches Institut of the University of Cologne, West Germany, where he is currently responsible for the development of millimeter- and sub-millimeter-wave receivers for radioastronomy and airborne radiometry.

Dr. Vowinkel is member of the Nachrichtentechnische Gesellschaft im VDE, West Germany.

Konrad Gruener was born in Munich, Germany, on July 9, 1939. He received the Diplom-Ingenieur degree in electrical engineering and the Doktor-Ingenieur degree, both from the Technical University of Munich, Munich, Germany in 1964 and 1970, respectively.

Since 1964, he has been with the Deutsche Forschungs- und Versuchsanstalt fuer Luft- und Raumfahrt (DFVLR) at Oberpfaffenhofen, Germany, where he has worked in the field of microwave antennas, synthesis of non-uniform waveguides, and microwave radiometry. He is presently head of the microwave radiometry division.

Werner Reinert was born in Jena, Germany, on April 25, 1943. He received the Diplom-Physiker degree and the Dr. degree from the University of Bonn, Bonn, Germany in 1969 and 1973, respectively.

From 1974 to 1980, he was with the Radioastronomisches Institut of the University of Bonn as a Research Assistant. He has worked in the development of sub-millimeter- and millimeter-wave heterodyne receiver systems used in radioastronomy research. His research activities have been concerned with Schottky-barrier diodes for low-noise cryogenic receivers. He also has been responsible for the developing of an airborne imaging system for millimeter waves. In 1981, he joined the Fraunhofer Institut für Angewandte Festkörperphysik, Freiburg, FRG, where he presently is engaged in the development of monolithic devices and integrated circuits for millimeter-wave receivers.